

# Quantification of MRI Sensitivity for Mono-disperse Microbubbles to Measure Subatmospheric Fluid Pressure Changes.

*Amgad Alrwaili, Martin Bencsik*

School of Science and Technology, Nottingham Trent University

Corresponding author: Martin Bencsik, Dept. of Physics and Mathematical Sciences  
College of Arts & Science, Nottingham Trent University  
Nottingham NG11 8NS, UK, E-Mail: martin.bencsik@ntu.ac.uk

## Abstract

It would be very beneficial to perform MRI of fluids and sense the fluid pressure changes. Our aim is to demonstrate a contrast agent capable of MR sensitivity to sub-atmospheric pressure changes. To achieve this, monodisperse microbubbles were prepared with an optically measured mean radius of  $1.4 \pm 0.8 \mu\text{m}$ . A repeated pressure change cycle was applied on the microbubble contrast agent, until it produced an MR signal change solely due to the bubble radius change. The bubbles' contribution to the relaxation rate before and after applying sub-atmospheric pressure changes was estimated and its echo time dependence modelled, so as to inform the mean radius change. The periodic subatmospheric pressure change was further applied until the MR signal change was only due to the bubble radius change. An excellent MR sensitivity of  $28 \text{ \% bar}^{-1}$  is demonstrated, bubble radii of  $2.4$  and  $1.8 \mu\text{m}$  are numerically estimated before and after the application of pressure, and the simulations are further used to estimate the optimum bubble radius maximising the MR sensitivity to a small change in radius.

## Keywords

MRI, Pressure, Diffusion, Contrast Agent, Microbubbles.

## 1. Introduction.

Mono-disperse microbubbles are known to be used in contrast agents, particularly within ultrasound imaging [1]. These agents usually consist of phospholipid coated gas filled bubbles within a water based suspending medium. They can be used as magnetic resonance (MR) pressure sensitive probes [2]. At the present time, measurement strategies are allowing the detection of pressures above atmospheric value by means of MRI, as was first demonstrated by Alexander [3] with a contrast agent comprising of microbubbles. The gas and liquid interface results in a high local polarising field gradient, due to the magnetic susceptibility step change. The application of sub-atmospheric pressure on the microbubbles increases the

bubbles' radii which is the source of the MR sensitivity that we measure. Subatmospheric pressures are relevant to many areas of research. In the medical field the carotid artery responses can be assessed by measuring sub atmospheric pressure of the lower body in the human vascular system [4]. In a different study, human exposure to subatmospheric pressure over a long time has been shown to cause a 'compartment syndrome' [5]. The water state exhibiting 'negative pressures' and its properties in plants soils has been studied in the context of the geochemistry of soil capillaries [6]. In this work, we demonstrate the MR sensitivity to sub-atmospheric pressure changes, and assess it by estimating the bubbles' contribution to the relaxation rate before and after pressure cycling.

## 2 Methods.

### 2.1 Microbubble Contribution to MR Relaxation.

Our quasi monodisperse microbubbles were prepared [7] with an optically measured mean radius of  $1.4 \pm 0.8 \mu\text{m}$ . A sample holder was made comprising two-compartments: one to accommodate a control gel originally made of 4 mL of 2% w/v gellan gel and 1mL of gas-free phospholipids solution, the other one to hold the contrast agent that consisted of 4 mL of gel, mixed with 1mL of phospholipids shaken sample (i.e. comprising of microbubbles). The sample receptacle was placed in the scanner and subjected to the MSME (Multi Slice Multi Echo) sequence of a Bruker BIOSPEC system, at field strength 2.35 T. The echo time  $T_E$  was systematically changed from 7 to 140 ms, to characterise the MR sensitivity. Matlab® homebuilt software was used to detect each compartment. The thermal noise was subtracted and a monoexponential decay curve was fitted to the compartments. The sensitivity was assessed by estimating the bubble contribution,  $R_2^{\text{bub}}$ , to the relaxation rate as discussed later in section 3.1.

### 2.2 MR Sensitivity to Subatmospheric Pressure Changes.

The same samples were used in this measurement, but the compartments were connected by a single tube with a T-junction, which was subsequently connected to a syringe pump (constant flow mode, flow rate = 30 mL/hr) and negative (-1 to 0 bar) fluid pressure gauge. The sub-atmospheric pressure cycle was continuously applied to both compartments at the same time. Using the MSME sequence with  $T_E = 10 \text{ ms}$ , the effective relaxation time,  $T_2^{\text{eff}}$ , of the contrast agent at rest was further measured, and found to be 194 ms. The RARE [8] sequence was subsequently used on the under pressurised samples with  $T_E = 10 \text{ ms}$ , RARE factor = image size, and  $T_E^{\text{eff}} = 2T_2^{\text{eff}}$  to optimise it to have a maximum sensitivity [9]. The pressure changes were cycled between 0 to -0.4 bars, until a stable MR signal change was obtained, due to bubble radius changes and free from bubble destruction artefacts [7].

## 3 Results.

### 3.1 Calculation of MR Sensitivity.

The relaxation rates in the contrast agent and in the control were both calculated and the difference yields the contribution that the microbubbles make to the contrast agent's overall relaxation rate. The MR sensitivity to the presence of bubbles will increase with longer echo time values, as is shown in Figure 1, before (highest curve, intact bubbles) and after (lower curve, due to bubble destruction) the pressure cycling. When the  $T_E$  value is decreased, the

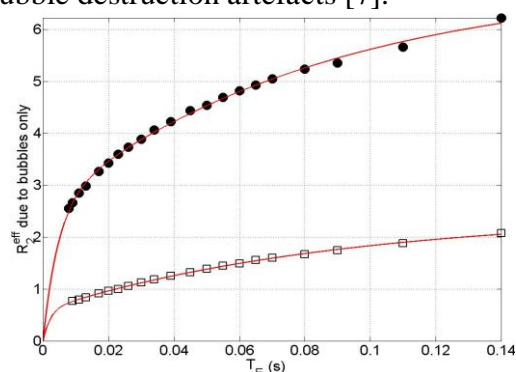


Figure 1. Contribution of the microbubbles to the relaxation rate shown as a function of the echo time before (●) and after (□) applying a pressure cycle.

resulting bubble relaxation rate ( $R_2^{\text{bub}}$ ), approaches zero, because the effect of the molecular diffusion is reduced to such an extent that the MR experiment becomes insensitive to the presence of bubbles. The variation of  $R_2^{\text{bub}}$  with  $T_E$  is well described by the following phenomenological biexponential recovery relationship,

$$R_2^{\text{bub}}(TE) = {}^1R_2^{\text{max}} \left( 1 - \exp\left(-\frac{TE}{TE_1^{\text{eff}}}\right) \right) + {}^2R_2^{\text{max}} \left( 1 - \exp\left(-\frac{TE}{TE_2^{\text{eff}}}\right) \right), \quad (1)$$

in which  ${}^1R_2^{\text{max}}$ ,  ${}^2R_2^{\text{max}}$ ,  $TE_1^{\text{eff}}$  and  $TE_2^{\text{eff}}$  are four constants to be fitted, and resulted in an effective curvature,

$$\frac{{}^1R_2^{\text{max}}}{{}^1R_2^{\text{max}} + {}^2R_2^{\text{max}}} \left( \frac{1}{TE_1^{\text{eff}}} \right) + \frac{{}^2R_2^{\text{max}}}{{}^1R_2^{\text{max}} + {}^2R_2^{\text{max}}} \left( \frac{1}{TE_2^{\text{eff}}} \right), \quad (2)$$

of 89 (before pressure cycling) and 121  $\text{ms}^{-1}$  (after pressure cycling) corresponding to [7] respective bubble radii of 2.4  $\mu\text{m}$ , and 1.8  $\mu\text{m}$ . The bubble density dropped by a factor 3 following the pressure cycling, as shown by the ratio of the curve's asymptotic values.

We also ran numerical simulations [7] to estimate  $R_2^{\text{bub}}$  for different bubble radii. In order to optimise MR-based pressure measurements, we need to establish the bubble radius which, when changed a little, will cause the largest change in  $R_2^{\text{bub}}$ . Towards shorter echo times, the value of  $R_2^{\text{bub}}$  tends to zero but it would be desirable to make its rate of change,

$$\frac{\partial R_2^{\text{bub}}}{\partial TE} = \frac{{}^1R_2^{\text{max}}}{TE_1^{\text{eff}}} \exp\left(-\frac{TE}{TE_1^{\text{eff}}}\right) + \frac{{}^2R_2^{\text{max}}}{TE_2^{\text{eff}}} \exp\left(-\frac{TE}{TE_2^{\text{eff}}}\right), \quad (3)$$

to be as large as possible. In Figure 2 we show the value of this quantity at echo time = 0. A pronounced maximum can be seen around a radius of 1.25  $\mu\text{m}$ .

### 3.2 Pressure and Bubble Radius Changes.

In the sub-atmospheric pressure measurement, the RARE sequence was set with  $T_E = 10$  ms, the contrast agent exhibited  $T_2^{\text{eff}} = 187$  ms, resulting in imaging done with RARE factor = 72 and  $T_E^{\text{eff}} = 374$  ms. The RARE image view of the dual-compartment vessel is shown in figure 3, with a clear negative contrast due to the presence of the bubbles in the compartment on the upper left view. For the data processing, each compartment was segmented. The top curve indicates the MR signal coming from the compartment with the control gel, (see Figure 3A) and demonstrates a hardware drift, but no MR sensitivity to the sub-atmospheric pressure changes (black square curve). The signal coming from thermal noise was further subtracted (baseline correction), and the signal

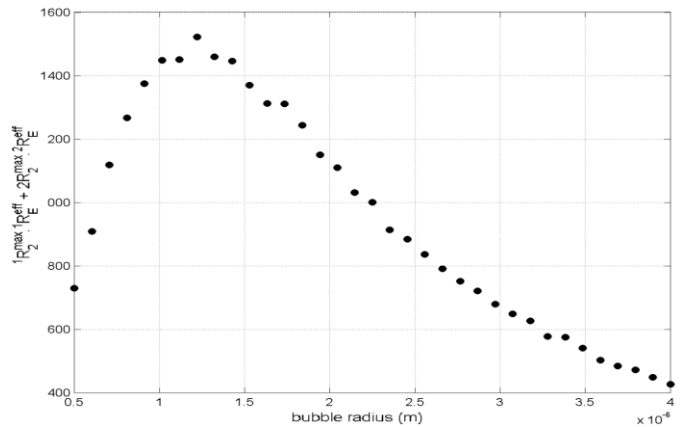
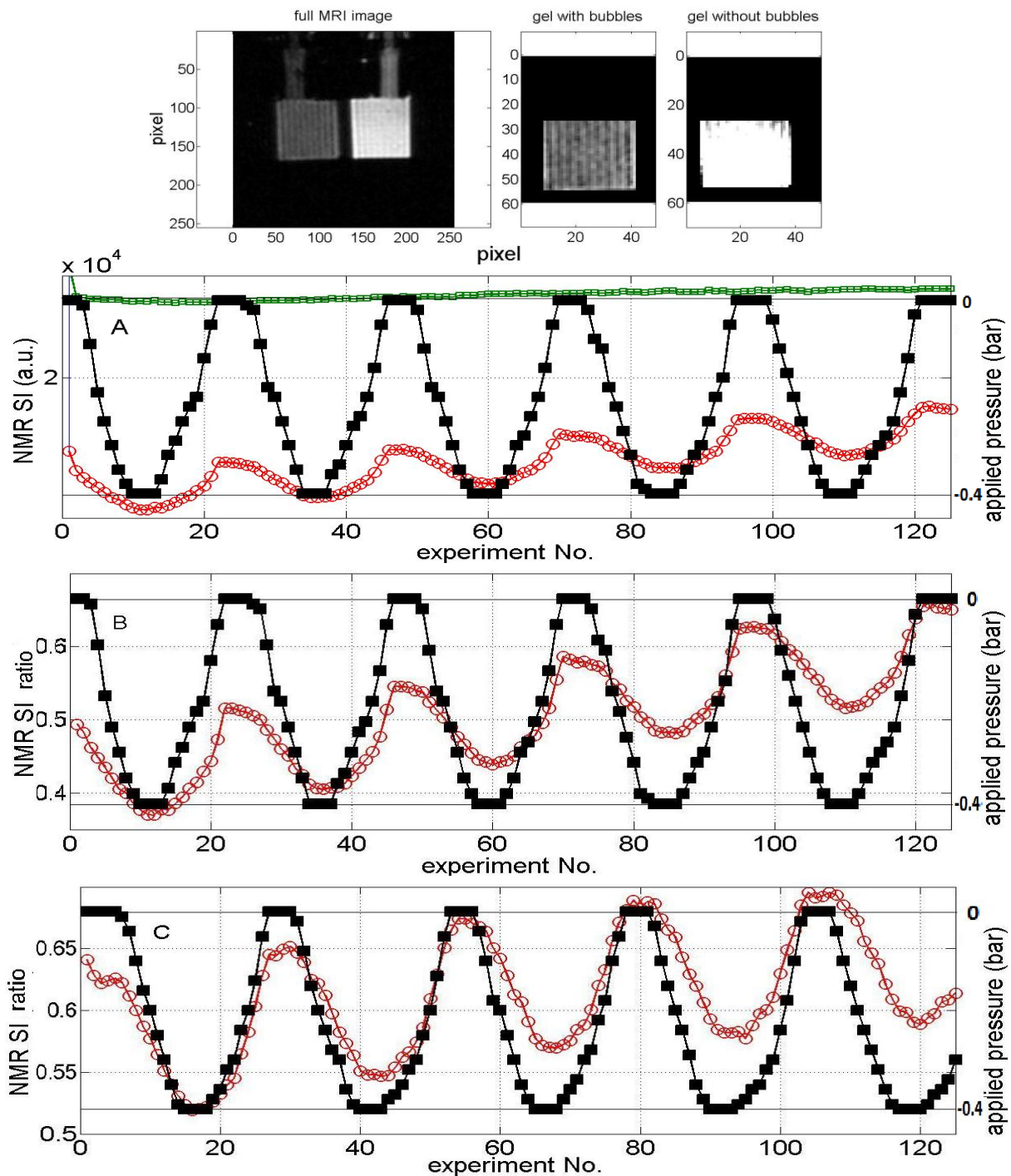


Figure 2. Numerical simulation results to establish the bubble radius optimizing MR signal change to bubble radius change.

from the contrast agent was divided by that of the control gel; the result can be observed in figure 3B with the compensated hardware drift. At the end of the first experiment, the shift in the sensitivity was noticeable; this was caused by bubble destruction due to the pressure. Ultimately, the MR sensitivity was 28%/bar. Then the measurements were replicated but with



**Figure 3:** Pressure variation experiments. **Top left:** RARE MRI image of the two-compartment sample holder, with good contrast due to microbubbles. **Top right:** selected FOV for the control (right) and contrast agent (left) used for the MR signal analysis shown in A, B and C. **Graph A:** time course of the measured pressure (black) and MR signal strength in the control gel (green line) and in the contrast agent (red curve) over 125 experiments, **Graph B:** same data, in which thermal noise has been subtracted, and in which the MR signal resulting from the contrast agent has been divided by the one resulting from the control gel. **Graph C:** a second measurement in which the RARE sequence has been re-optimised to the fluid's  $T_2^{\text{eff}}$  value, reached at the end of the first experiment, and MR sensitivity drift is minimal at the end of this measurement.

a new  $T_2^{\text{eff}}$  evaluation (238 ms), the RARE experiment was repeated with an updated RARE factor = 92,  $T_E^{\text{eff}} = 476$  ms, and the sub-atmospheric pressure cycle was applied again (see Figure 3C), yielding the same optimum sensitivity until the very last pressure cycle. The substantially reduced sensitivity drift indicates an MR signal change mostly due to bubble radius change, although the effect of further ageing of the microbubbles can still be seen.

#### 4. Conclusion.

We have demonstrated an MRI experiment in which subatmospheric pressures have been interrogated by means of a microbubble-based contrast agent. We have assessed the MR sensitivity prior to and after application of a regular pressure cycle, and have demonstrated a signal change due to the bubble radius change only. The bubble destruction results in a shift in the bubble mean radius which we have estimated.

In the future this experimental setup will be used to cycle pressure above and below atmospheric value to further quantify the associated MR sensitivity. It is anticipated that in the future mono-disperse bubble based contrast agents will be useful in the fields of biomedical and biology MRI.

#### Acknowledgements

We are most grateful to Professor Peter Morris from the University of Nottingham for donating the Bruker system to us and to Dr. Malcolm Prior and Dr. John Owers-Bradley for their help in re-siting the system. We would like to acknowledge Jonathan McKendry, and Stephen Evans from Leeds University who provided us the methodology to generate the microbubbles. We would like to acknowledge David Fairhurst, Robert Morris, Victoria Mundell and Gareth Cave, for their help. We would like to thank the Saudi Arabian Government for funding Mr. A. Al-Rwaili's Ph.D. bursary to undertake this work.

#### References.

- [1] A. L. Klibanov, "Microbubble contrast agents - targeted ultrasound imaging and ultrasound-assisted drug delivery applications," *Investigative Radiology*, vol. 41, no. 3, pp. 354–362, 2006.
- [2] R. Dharmakumar, D. Plewes, and G. Wright, "On the parameters affecting the sensitivity of MR measures of pressure with microbubbles," *Magnetic Resonance in Medicine*, vol. 47, no. 2, pp. 264–273, 2002.
- [3] Alexander A.L., et al., Microbubbles as novel pressure-sensitive MR contrast agents. *Magnetic Resonance in Medicine*, 1996; 35:801-806.
- [4] C. M. Brown, et al., Effects of Lower Body Negative Pressure on Cardiac and Vascular Responses to Carotid Baroreflex Stimulation. *Physiol. Res.* 52: 637-645, 2003.
- [5] Bluman, Eric M., et al., Subatmospheric Pressure-Induced Compartment Syndrome of the Entire Upper Extremity. *Journal of Bone and Joint Surgery*, Volume 86A (9): 2041-2044, 2004.
- [6] L. Mercury, and Y. Tardy, Negative pressure of stretched liquid water. *Geochemistry of soil capillaries*, *Geochimica et Cosmochimica Acta*, Vol. 65, No. 20, pp.3391–3408, 2001.
- [7] M. Bencsik, et al., Quantitation of MRI sensitivity to monodisperse microbubble contrast agents for spatially resolved manometry, *Mag. Res. Med.*, published online Dec 2012, DOI: 10.1002/mrm.24575.
- [8] J. Hennig et al., RARE imaging - a fast imaging method for clinical MR, *Magn. Reson. Med.* 3 (1986) 823-833.
- [9] R. H. Morris, et al., Robust spatially resolved pressure measurements using MRI with Novel buoyant advection-free preparations of stable microbubbles in polysaccharide gels, *Journal of Magnetic Resonance* 193 (2008) 159– 167.